ANS RPSD 2018 - 20th Topical Meeting of the Radiation Protection & Shielding Division of ANS
Santa Fe, NM, August 26 – 31, 2018, on CD-ROM, American Nuclear Society, LaGrange Park, IL (2018)

WATTS BAR I EX-CORE ANALYSES USING VERA

[1*]E. Davidson, T. Pandya, A. Godfrey, and M. Asgari

*One Bethel Valley Road, Oak Ridge, TN, 37831, 865-576-0575, and *davidsonee@ornl.gov*

The integration and direct coupling of the Oak Ridge National Laboratory (ORNL) Shift Monte Carlo code within the Consortium for Advanced Simulation of Light Water Reactors (CASL) Virtual Environment for Reactor Applications (VERA) offers unique capabilities that combine high-fidelity in-core and ex-core radiation transport. In this recent development activity, the deterministic neutronics code MPACT performs the in-core radiation transport with temperature feedback using COBRA-TF (CTF), and provides the fission source to Shift for a follow-on fixed source radiation transport calculation to determine ex-core quantities of interest. The coupling of MPACT to Shift allows the neutron source for the ex-core transport to be calculated from the time-dependent, fully coupled MPACT solution. This paper presents the first use of VERA to perform coupon irradiation for validation of its ex-core capabilities.

I. EX-CORE RADIATION TRANSPORT MODELING WITH VERA

VERA [1] has been extended to perform ex-core calculations with the Shift [2] Monte Carlo code. The in-core transport with temperature feedback is performed by coupled MPACT [3] and COBRA-TF (CTF) [4] calculations, while the fluence or detector response calculations outside the core barrel are performed by Shift. The ex-core region is defined using Shift's general geometry package, also known as Omnibus general geometry (GG), while the in-core geometry is defined using the standard VERA input.

For these ex-core calculations, VERA launches MPACT/CTF on a fixed number of processors for user-specified state points. After completing MPACT/CTF calculations for each state point, VERA launches an independent Shift fixed-source calculation on a separate set of processors for ex-core calculations. These fixed-source Shift calculations can be performed in forward mode with no variance reduction (VR) or with Consistent Adjoint-Driven Importance Sampling (CADIS). Incorporation of CADIS in VERA is still under active development. ORNL's discrete ordinates solver, Denovo [5], which is part of the Exnihilo code suite, is used to calculate the space- and energy-dependent weight windows for Shift. The CADIS methodology also produces source biasing parameters that are consistent with the weight windows. The biased source implementation is under development in VERA/Shift and will be implemented soon. These VR parameters significantly reduce tally variances. More details regarding CADIS can be found in [6] to [8].

More details about the MPACT/Shift coupling can be found in Pandya et al., "Excore Radiation Transport Modeling with VERA: Manual" [9]. MPACT/CTF can pass detailed isotopics and temperatures within all regions in the core to Shift, but due to memory constraints, only the pin-wise fission source is passed to Shift for the calculations in this paper. Currently, Shift samples from the fission source provided by MPACT and runs a fixed-source calculation to determine ex-core quantities of interest. The fission source passed from MPACT to Shift provides only the spatially-dependent source without the energy distribution of the source. Due to memory constraints, the energy-dependent spatial fission source is not passed to Shift, and Shift assumes a ^{235}U Watt spectrum to sample from the source. Also, as a consequence of only passing the fission source from MPACT to Shift, Shift sets the composition of the fuel within the core to the initial state specified in the VERA common input for the full calculation.

The fixed-source transport can be run in neutron-only (n) or neutron-photon (n-γ) modes. For coupled (n-γ) problems, the secondary gamma source is sampled from neutron interactions within the core elements during neutron transport. Shift does not currently support prompt fission gammas or delayed fission product gammas as sources in a fixed-source calculation. Shift performs all ex-core calculations using continuous-energy (CE) physics. Multigroup physics is required to run the adjoint Denovo calculation for generation of the VR parameters using the CADIS methodology. Once the adjoint solution has been calculated by Denovo, the detailed ex-core transport is

[1] Notice: This manuscript has been authored by UT-Battelle, LLC, under contract DE-AC05-00OR22725 with the US Department of Energy (DOE). The US government retains and the publisher, by accepting the article for publication, acknowledges that the US government retains a nonexclusive, paid-up, irrevocable, worldwide license to publish or reproduce the published form of this manuscript, or allow others to do so, for US government purposes. DOE will provide public access to these results of federally sponsored research in accordance with the DOE Public Access Plan (http://energy.gov/downloads/doe-public-access-plan)

performed by Shift using CE physics and the weight windows generated by Denovo.

VERA provides users with the unique opportunity to take advantage of advanced simulation methods to calculate time-dependent and fully coupled solutions for coupon fluence, pressure vessel fluence, and ex-core detector responses for multiple cycles, each of which can contain a user-specified number of state points. These state points are static short timestep calculations that simulate a full cycle. This paper demonstrates VERA's abilities to perform coupon irradiation calculations. A simple quarter core ex-core region was set up for Watts Bar Unit I, and the flux, and iron displacement per atom (dpa) rates for the first two cycles are presented in this paper. These results were all obtained with Shift in forward mode without any hybrid capabilities invoked. These results are compared to the results presented in a public US Nuclear Regulatory Commission (NRC) report for Watts Bar I [10]. Results from calculations that take advantage of Shift's hybrid capabilities—i.e., CADIS—have been omitted from this paper but will be presented at the conference, along with results from cycle 3.

II. OMNIBUS EX-CORE MODEL

A simplified 3D ex-core model for a quarter core Watts Bar Unit I VERA model was set up using Omnibus' GG input format. This ex-core region was modeled based on the VERA input for CASL progression problem 7 for Watts Bar Unit I [11]. The simplified ex-core model contains 2 power range detectors (top and bottom) and a single surveillance capsule with ^{238}U, iron (Fe), and copper (Cu) coupons in the northeast quadrant. More details regarding this model and the modeling workflow can be found in Davidson et al. [12].

All of the reactor geometry from the center of the core to the barrel's inner radius in the radial direction, and from the lower to upper core plates in the axial direction, is generated using the VERA common input with minimal user effort in Shift's GG input. Only the geometry and material compositions for regions outside the barrel's inner radius are explicitly defined in the GG input, giving the user great flexibility in modeling complex ex-core features. Finally, tallies in various regions of interest are set up in the GG input file to analyze detector response and to calculate fluence in the coupons.

Figure 1 shows an image of the simplified model with a power range detector and a single surveillance capsule located in the northeast quadrant generated with a raytrace of the material compositions in the model.

A cell's raytrace can be performed while setting up the ex-core model with a dummy core (orange region in Figure 3) to ensure that there are no user-input geometry errors. Once the user is confident that the ex-core model is accurate, a VERA calculation is performed from which the output files produced by Shift are used to generate the image shown in Figure 1. The modeling, plotting, and calculation steps are discussed in more detail in subsequent sections.

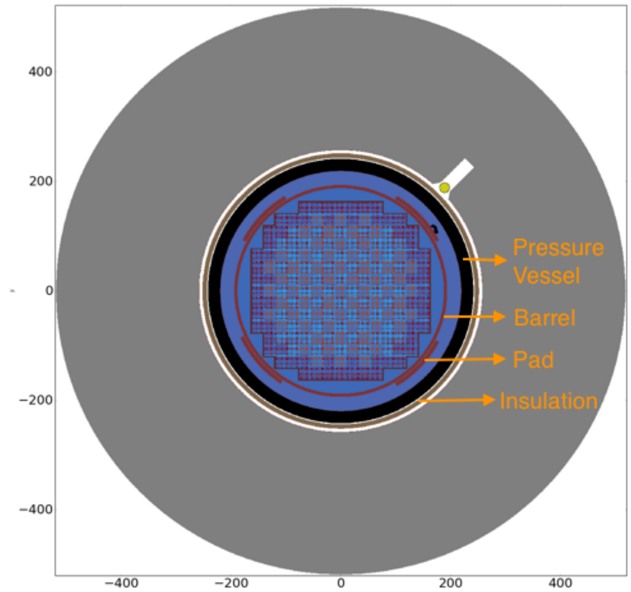

Fig. 1. Simplified model: axial slice at z = 200 cm (image shows material compositions).

Figures 2 and 3 show images of the model generated with a raytrace of the individual cells in the model. Figure 2 shows the three coupons in the single surveillance capsule: ^{238}U, natural Fe, and natural Cu.

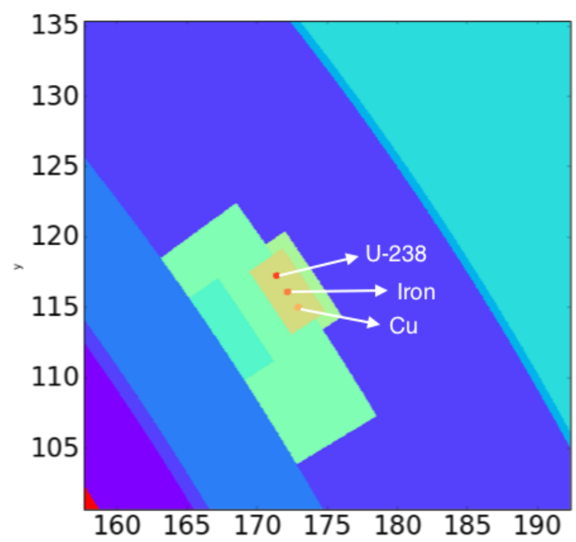

Fig. 2. Closer view of coupons in the single surveillance capsule in the simplified model: axial slice at z = 200 cm (image shows individual cells in the geometry).

The relative scale and location of the surveillance capsule and the power range detector can be seen in Figure 3.

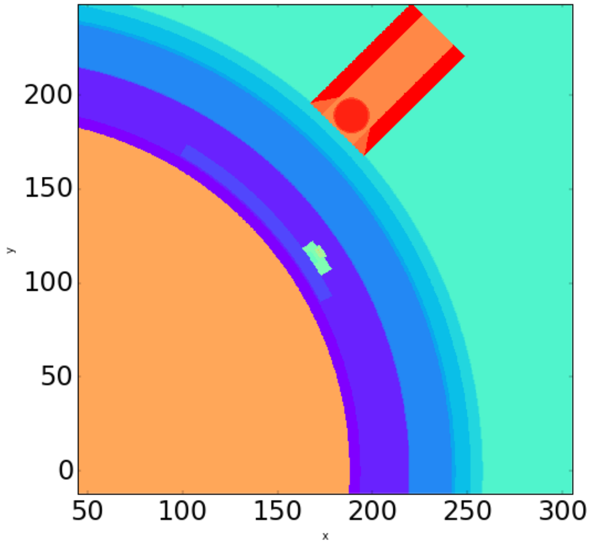

Fig. 3. View of the single surveillance capsule and the power range detector in the simplified model: axial slice at z = 200 cm (image shows individual cells in the geometry).

III. MODELING WORKFLOW

Setting up an Omnibus GG input is similar to setting up geometry with KENO in SCALE [13] or with MCNP [14]. The learning curve associated with setting up the GG input is not as steep if the user is familiar with setting up an input for combinatorial geometry. However, the steps required to view the geometry and the output require advanced user knowledge in Python scripting, the matplotlib plotting package, and HDF5-file reading/parsing. The geometry and all the results are processed in Jupyter notebooks. Jupyter notebook is an open-source web application available through *jupyter.org*. It allows users to create code and visualize results in an interactive environment.

III.A. Setting up GG input

The first step in the modeling process is to set up and test the ex-core geometry in GG. During this initial phase, VERA is not run, so the core that is set up in the VERA input is unknown to Shift. Therefore, this core region is replaced with a so-called "fake core" in the GG input during the initial modeling phase only. This fake core fills the region within the inner barrel (the orange region in Figure 3) with the following example lines of GG input.

```
[UNIVERSE=general reactor]
boundary "inner_barrel"

[UNIVERSE][SHAPE=cyl inner_barrel]
radius 187.96
extents -5.0 413.937
origin 0 0 0
axis z

[UNIVERSE][CELL fake_core]
comp fake_core
shapes -inner_barrel
```

This core is then filled in a HOLE, similar to KENO geometry, using the following lines of input:

```
[UNIVERSE][HOLE thecore]
fill reactor
```

The barrel, pads, surveillance capsules, downcomer region, pressure vessel, insulation, air gaps, and concrete shield are all modeled in the GG input to enable ex-core Monte Carlo transport with Shift. These regions are modeled using *SHAPE*, *CELL*, and *HOLE* blocks, similar to KENO geometry. Their material compositions are also explicitly defined in the GG input when running VERA. Detailed instructions on setting up various shapes and defining cells and holes are provided in the Exnihilo Transport Code Manual [15].

The *gg2xml* executable is used to convert this ASCII GG input during this initial modeling phase to an XML input. This is done by simply invoking the following command in the terminal window:

```
./gg2xml ex-core_input_filename.omn
```

This creates an *ex-core_input_filename.gg.xml* file which can be pulled into a Jupyter notebook to allow viewing of the geometry (example plots from these notebooks shown in Figures 1–3). The raytrace is done when the user invokes the imager through the Jupyter notebook.

III.B. Running GG input through VERA

The second step in the modeling process is to run the Omnibus GG input through VERA. To perform this step, the fake core definition shown in the previous section is removed from the input and is replaced with the following line to integrate the VERA core geometry and the Omnibus GG ex-core geometry.

```
[UNIVERSE=core reactor]
```

Next, an additional *translate* parameter is specified within the reactor HOLE (shown in the previous section) to move the VERA core origin to correspond with the origin in the GG input. With this additional parameter, the *HOLE* is defined as:

```
[UNIVERSE][HOLE thecore]
fill reactor
translate -241.70 -241.70 0.0
```

This translation corresponds to the outer radius of the pressure vessel. Figure 4 shows the VERA origin with a red dot and the Shift origin with a blue dot. The origin of the GG input is defined by the Omnibus input. For this problem, the GG origin is located at (0, 0, 0), conforming to Shift's origin. If the outer radius of the pressure vessel is 241.70 cm, then the core must be translated by (-241.70, -241.70, 0) for the VERA core origin to correspond with the Shift origin. This can be a source of user input error, so close attention should be given to the translation when setting up the Omnibus and VERA inputs. Note that if the GG origin is defined to correspond with the VERA origin, then no translation is necessary. However, in this case, the user must set the origin for each shape in the GG input to correspond to VERA's origin. For example, the origin would be (241.70, 241.70, 0) for the example provided here.

As in the *gg2xml* executable, the *excore2xml* executable is run and included in the same portable batch system (PBS) job submission script that is used to run VERA. This executable generates an XML file containing all the ex-core geometry, ex-core composition, and tally information from the GG input. The only difference between *gg2xml* and *excore2xml* is that *gg2xml* only converts the geometry without any compositions or tallies. This helps the user to focus on constructing the geometry accurately.

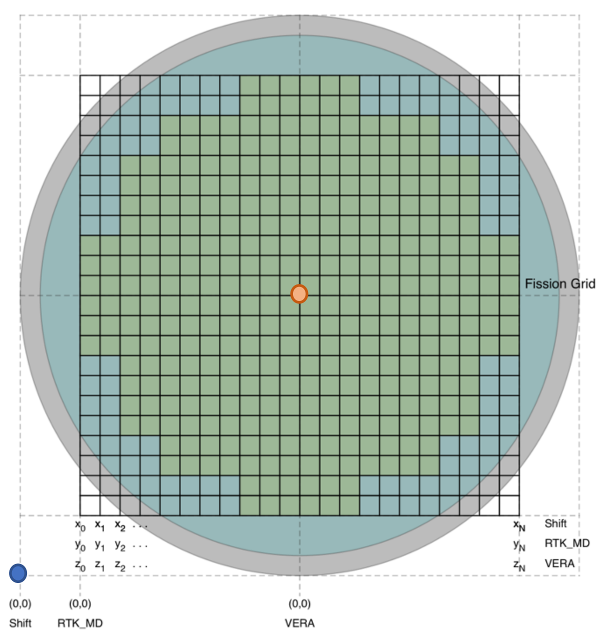

Fig 4. VERA, Shift, and Reactor ToolKit (RTK) origin relationships. (RTK is the inherent geometry Shift uses for the in-core geometry from VERA common input.)

IV. RESULTS

Once VERA and GG inputs are set up and VERA has successfully run to completion, the HDF5 outputs can be processed with a Jupyter notebook.

Preliminary results are presented here for Watts Bar Unit I cycles 1 and 2 for neutron flux in the iron coupon located at the center of the single surveillance capsule (Tables II and III), and the iron dpa rates at this location (Table I). It is assumed that the total height of the iron coupon is 20 cm, and it is axisymmetric about the active core mid-plane. The iron dpa rates are calculated using the response function provided in ASTM E693-17 [16] for neutrons. The detailed power history and burnup for cycles 1 and 2 used in this calculation cannot be presented here for proprietary reasons. The results generated for this work are compared with the results presented in BWXT's "Part 1 – Watts Bar Nuclear Plant Unit 1, Reactor Vessel Surveillance Capsule W Test Results & Reactor Vessel Fracture Toughness (J-R) Test Results" [10].

Before presenting the results, it is important to discuss some key differences in the data and the methods used to generate the BWXT [10] and VERA results. The iron displacement rates generated by VERA used the latest response functions from ASTM E693-17 published in 2017, whereas the reference results were generated using ASTM E693-94 published in 2001. ASTM E693-17 [16] discuses differences seen in iron dpa rates using different response functions generated in the past for ASTM E693. Although the iron displacement cross sections have changed by about 60% in the energy region around 10 keV, 10% for energies between 100 keV and 2 MeV, and a factor 4 near 1 keV in the current release, the integral iron dpa values are less sensitive to the changes in the cross section [16]. These differences are discussed in detail in [16].

In addition to the differences in the response function used to generate the iron dpa rates, there are differences in the cross-section libraries used to run the codes. In the BWXT results [10], the BUGLE-96 library with 47 neutron energy groups derived from ENDF/B-VI data was used with the DORT [17] two-dimensional discrete ordinates code. The transport calculations for Watts Bar Unit I were generated using R-θ and R-Z models. Further details on the radial and axial meshes used in DORT to generate the reference results can be found in [10]. In VERA, MPACT uses a 51-neutron-group library based on ENDF/B-VII to perform a detailed pin-wise solution with thermal feedback (CTF) for the in-core radiation transport. MPACT is a 2D-MOC (radial) and 1D-nodal (axial) methods code. Shift uses the CE SCALE library based on ENDF/B-VII to perform the fixed source transport calculation. The differences in the data, the methods, and the assumptions made to set up the model for Watts Bar Unit I in the BWXT analysis and the current VERA analysis will lead to differences in the results. The relative differences between VERA and the reference BWXT results are discussed next.

Tables I to III show the time-averaged flux and iron dpa rates. There were 32 depletion state points in the Watts Bar Unit I cycle 1 model with Shift running 1 billion particles per state point (in forward mode with no VR), took about 30 hours to finish running on 1,600 cores (840 cores for MPACT and 760 cores for Shift). There were 22 depletion state points in the Watts Bar I cycle 2 model, with Shift running 0.75 billion particles at each state point. This calculation took 24 hours to complete on 1,344 cores. The performance of these calculations is expected to increase significantly with the incorporation of a fully functional CADIS option in VERA.

Table I shows that the VERA results differ by approximately 6% for cycle 1 and 21% for cycle 2 from the BWXT results. Table II shows that there is a 6% difference for cycle 1 and an 8% difference in cycle 2 neutron flux for neutron energies greater than 1 MeV between VERA and BWXT results. Table III shows 12% and 25% differences in cycles 1 and 2 between VERA and BWXT results for neutron energies greater than 0.1 MeV. The relative differences are the largest for neutron flux greater than 0.1 MeV.

TABLE I. Iron displacements per atom rates (dpa/s)

Cycle	VERA (1σ %Relative Error)	Reference Results [10]
1	2.21×10^{-10} (6.5%)	2.35×10^{-10}
2	1.27×10^{-10} (6.2%)	1.61×10^{-10}

TABLE II. Neutron Flux (E > 1.0 MeV) n/(cm^{2}s)

Cycle	VERA (1σ %Relative Error)	Reference Results [10]
1	1.07×10^{11} (5.5%)	1.13×10^{11}
2	7.22×10^{10} (10%)	7.84×10^{10}

TABLE III. Neutron Flux (E > 0.1 MeV) n/(cm^{2}s)

Cycle	VERA (1σ %Relative Error)	Reference Results [10]
1	4.89×10^{11} (2.9%)	5.59×10^{11}
2	2.83×10^{11} (5.4%)	3.79×10^{11}

The data used to perform the calculations in the BWXT tests [10] and VERA could be a potential source of differences seen in the results. In addition to the differences in the data, there are differences in the BWXT and VERA models. They are discussed in detail in [10], however, a few of these differences are highlighted here. The BWXT core region homogenized the fuel, cladding and water. The average core water temperature was used to define the water density in the entire core. VERA models every pin in an assembly and the water density changes with the temperature-feedback calculations performed by CTF. The ex-core VERA calculations by Shift assume that fuel compositions for each cycle begin with the compositions at the first state point. For cycle 1, Shift assumes fresh fuel to perform ex-core calculations using the spatially-dependent fission source and a ^{235}U Watt spectrum to sample the neutron location and energy for each user-defined state point. Shift assumes the fuel compositions for each pin at the end of cycle 1 to perform cycle 2 calculations with the spatially-dependent fission source and ^{235}U Watt spectrum at each user-defined state point in cycle 2. Assuming a ^{235}U Watt spectrum to sample the starting neutron energy beyond the first cycle as other fissionable nuclides (i.e., ^{239}Pu) build up may contribute to some differences. The BWXT results account for fission spectrum contributions from ^{235}U, ^{238}U, ^{239}Pu, ^{240}Pu and ^{241}Pu.

Plant-specific pin power distributions for Watts Bar Unit I were not available when the BWXT results were generated, therefore results in [10] were generated using pin power distributions from another Westinghouse PWR. Plant specific data have been taken into account to generate the time-dependent pin power distributions using VERA for each user-defined state point for cycles 1 and 2.

The BWXT results were generated using R-θ and R-Z DORT models. Although the R-θ DORT model accounted for the surveillance capsules and the pads, the R-Z model did not include the neutron pad, surveillance capsules or the former plates. The iron dpa rates and the flux reported in the iron coupon located at the center of the single surveillance capsule in the VERA model is 20 cm long and is axisymmetric about the core midplane. This could be a reason why there is a negative bias in the VERA results with respect to the BWXT results.

The BWXT results also only took into account a single axial power shape for all the fuel cycles, whereas VERA took into account the pin-wise spatially-dependent (radially and axially defined) fission source for each state point in each cycle.

The effects of some of these assumptions may be minor, but they are highlighted here to provide the reader with some context on the differences in the models. As discussed earlier, the VERA results were obtained from Shift with no CADIS VR parameters. This means that the variances in the tallied results at individual state points were high and can be reduced with CADIS. These results will be regenerated once CADIS is available in VERA for user testing. The new results from CADIS will also be examined for VERA's performance when running with hybrid capabilities.

V. CONCLUSION AND FUTURE WORK

VERA results were generated for this paper with MPACT/CTF performing a fully coupled, temperature-dependent in-core radiation transport calculation after which the spatially dependent fission source is passed to Shift for a follow-on Monte Carlo calculation that tallies flux and iron dpa rates in the single surveillance capsules. This paper demonstrates the successful coupling of MPACT/CTF and Shift for ex-core calculations. While additional development is needed to refine these calculations, the results from this initial analysis with VERA are promising. Most differences between the BWXT and VERA results arise due to varying assumptions and methods used to build the models to calculate the exposure rates. Specifically, deterministic methods were used to generate the reference results in BWXT tests [10], whereas Monte Carlo (with no VR) was used to generate the VERA results. In addition to the differences in the methods used to generate the results, the data used to run VERA and DORT in the BWXT tests [10] are different, and the assumptions used to model the cores are different. These differences in radiation transport methods, data and models will lead to differences in the results.

Further investigations on flux and iron dpa rates are currently being performed with Watts Bar I cycle 3 models. More results with coupon reaction rates provided in the BWXT results [10] will be generated with VERA using CADIS, and these results will be presented at the conference. Future work involves further user testing, code validation, and providing feedback to the developers to facilitate user friendly input setup and execution of ex-core problems in VERA.

ACKNOWLEDGMENTS

The authors would like to acknowledge the user support provided by the Exnihilo and MPACT code development teams for this work.

This research was supported by the Consortium for Advanced Simulation of Light Water Reactors (http://www.casl.gov), an Energy Innovation Hub (http://www.energy.gov/hubs) for Modeling and Simulation of Nuclear Reactors under U.S. Department of Energy Contract No. DE-AC05-00OR22725. This research also used resources of the Compute and Data Environment for Science (CADES) at the Oak Ridge National Laboratory, which is supported by the Office of Science of the U.S. Department of Energy

REFERENCES

1. J. A. Turner et al., "The Virtual Environment for Reactor Applications (VERA): Design and architecture," *J. Comput. Phys.*, **326**, 544–568 (2016).

2. T. M. Pandya, S. R. Johnson, T. M. Evans, G. G. Davidson, S. P. Hamilton, and A. T. Godfrey, "Capabilities, Implementation, and Benchmarking of Shift, a Massively Parallel Monte Carlo Radiation Transport Code," *J. Comput. Phys.*, **308**, 239–272 (2016).

3. B. Collins et al., "Stability and Accuracy of 3D Neutron Transport Simulations Using the 2D/1D Method in MPACT," *J. Comput. Phys.*, **326**, 612 (2016).

4. R. K. Salko and M. N. Avramova, "CTF Theory Manual," The Pennsylvania State University (2012).

5. S. P. Hamilton, T. M. Evans, G. G. Davidson, S. R. Johnson, T. M. Pandya, and A. T. Godfrey, "Hot Zero Power Reactor Calculations Using the Insilico Code," *J. Comput. Phys.*, **314**, 700–711 (2016).

6. J. C. Wagner, D. E. Peplow, S. W. Mosher, and T. M. Evans, "Review of Hybrid (Deterministic/Monte Carlo) Radiation Transport Methods, Codes, and Applications at Oak Ridge National Laboratory." *Joint International Conference on Supercomputing in Nuclear Applications and Monte Carlo (SNA + MC2010)*, Tokyo, Japan, October 17–21, 2010.

7. M. A. Cooper and E. W. Larsen, "Automated Weight Windows for Global Monte Carlo Particle Transport Calculations," *Nucl. Sci. Eng.*, **137**, 1–13 (2001).

8. J. C. Wagner, D. E. Peplow, and S. W. Mosher, "FW-CADIS Method for Global and Semi-Global Variance Reduction of Monte Carlo Radiation Transport Calculations," *Nucl. Sci. Eng.*, **176**, 37–57 (2012).

9. T. Pandya, T. Evans, K. Clarno, and B. Collins, "Excore Radiation Transport Modeling with VERA: Manual," Radiation Transport Methods, Consortium of Advanced Simulation of LWRs (CASL), CASL-U-2018-1556-0000 (2018).

10. BWXT Services Inc., "Part 1 – Watts Bar Nuclear Plant Unit 1, Reactor Vessel Surveillance Capsule W Test Results & Reactor Vessel Fracture Toughness (J-R) Test Results," NRC Public Document, ML012900048 (2001).

11. A. Godfrey, "VERA Core Physics Benchmark Progression Problem Specifications," Physics Integration, Consortium for Advanced Simulation of LWRs (CASL), CASL-U-2012-0131-004 (2014).

12. E. Davidson, T. Pandya, A. Godfrey, and T. Evans, "Testing of Omnibus General Geometry Models for Ex-Core Applications in VERA," Consortium for

Advanced Simulation of LWRs (CASL), CASL-U-2018-1561-0000 (2018).

13. B. T. Rearden and M. A. Jessee, Eds., SCALE Code System, ORNL/TM-2005/39, Version 6.2, UT-Battelle, LLC, Oak Ridge National Laboratory (2016). Available from Radiation Safety Information Computational Center as CCC-834.
14. X-5 Monte Carlo Team, *MCNP – A General Monte Carlo N-Particle Transport Code, Version 5*, LA-CP-03-0284, Los Alamos National Laboratory (2003).
15. S. Johnson, T. Evans, G. Davidson, S. Hamilton and T. Pandya, "Exnihilo Transport Code Manual," Release 6.2.0 (Dev), Oak Ridge National Laboratory (2017).
16. ASTM E693-17, "Standard Practice for Characterizing Neutron Exposures in Iron and Low Alloy Steels in Terms of Displacements per Atom (DPA)," ASTM International, West Conshohocken, PA (2017).
17. RSICC Computer Code Collection, "TORT-DORT-PC, Two- and Three-Dimensional Discrete Ordinates Transport Version 2.7.3," CCC-543, available from the Radiation Safety Information Computational Center, Oak Ridge National Laboratory, Oak Ridge, TN (1996).